Annals of Occupational Hygiene Advance Access published October 14, 2006

Ann. Occup. Hyg., pp. 1–8

doi:10.1093/annhyg/mel067

Comparison of the Grimm 1.108 and 1.109 Portable Aerosol Spectrometer to the TSI 3321 Aerodynamic Particle Sizer for Dry Particles

THOMAS M. PETERS*, DARRIN OTT and PATRICK T. O'SHAUGHNESSY

Department of Occupational and Environmental Health, The University of Iowa, 100 Oakdale Campus, 102 IREH Iowa City, IA 52242-5000, USA

Received 11 May 2006; in final form 8 August 2006

This study compared the response of two optical particle counters with that of an aerodynamic particle sizer. The optical particle counters rely on the amount of incident light scattered at 90° by a particle to measure particle number concentration by optical particle size. Two models of optical particle counters from Grimm Technologies were used: the portable aerosol spectrometer (PAS) 1.108 (0.3–20 μm in 15 channels); and the PAS 1.109 (0.2–20 μm in 30 size channels). With a substantially different operating principle from that employed by the optical particle counters, the aerodynamic particle sizer (APS) model 3321 (TSI, Inc., St Paul, MN, USA) sizes particles according to their behavior in an accelerating flow to provide particle number concentration by aerodynamic size over a slightly narrower size range (0.5–20 μm) in 52 channels. The responses of these instruments were compared for three sizes of monodisperse solid aerosols composed of polystyrene latex spheres and a polydisperse aerosol composed of Arizona test dust. The PASs provided similar results to those from the APS. However, there were systematic differences among instruments in number and mass concentration measurement that depended upon particle size.

Keywords: aerodynamic particle size; particle size; performance evaluation

INTRODUCTION

Worldwide, exposure to ambient particulate air pollution has been associated with ~3% of mortality from cardiopulmonary disease, 5% of mortality from cancer of the trachea, bronchus and lung, and 1% of mortality from respiratory infections in children (Cohen *et al*., 2005). Particle concentration by size is a key determinant of the ability of a particulate exposure to elicit such adverse health effects (Schlesinger *et al*., 2006). Some adverse health effects, particularly those related to cardiovascular function, appear to be related to short-term changes in particle concentration by size (Peters *et al*., 2001; Janssen *et al*., 2002; D'Ippoliti *et al*., 2003; Wellenius *et al*., 2005). Thus, assessment of particle exposures often requires instruments that provide a fairly rapid measure of particle concentration by size.

Optical particle counters provide rapid measurement of particle number concentration by optical size from roughly 0.2–30 μm. In an optical particle counter, each particle is sized by the amount of incident light scattered (Gebhart, 2001). Proper sizing may be ensured by the use of monodisperse polystyrene latex (PSL) and proper mass correlation may be established by the use of polydisperse dust. The density correlation may be established by mass correlation found in the environment (Hinds, 1999). Grimm Technologies, Inc. (Douglasville, GA, USA) offers two compact optical particle counters: the portable aerosol spectrometer (PAS) 1.108 and the PAS 1.109. These instruments have found use in diverse applications that range from vertical profiling of airborne particulate matter (Colls and Micallef, 1999), to evaluating tractor cab aerosol protection factors (Hall *et al*., 2002), to estimating respirable dust concentration in occupational settings (Peters *et al*., 2005). However, only a single study was found in peer-reviewed literature to document their performance. In this study, Teikari *et al*. (2003) found that the mass concentration

*Author to whom correspondence should be addressed.
E-mail: thomas-m-peters@uiowa.edu

by size measured with a PAS 1.105, an earlier model PAS than those mentioned above, compared favorably with that measured with a cascade impactor for quartz dust.

Alternatively, time-of-flight instruments may be used to obtain particle number concentration by aerodynamic size over a size range similar to that of optical particle counters. In a time-of-flight instrument, an aerosol is accelerated through a nozzle, and particles lag behind the carrier gas because of their inertia. Particles are sized according to the time that they take to traverse two laser beams (i.e. the time-of-flight) near the nozzle outlet, with larger particles having longer time-of-flights. In contrast to the optical particle counters mentioned above, the performance of the time-of-flight instrument used in this study, the Aerodynamic Particle Sizer (APS) model 3321 (TSI, Inc., St Paul, MN, USA), has been documented in more than 25 peer-reviewed journal articles (Baron *et al*., 2001). Volckens and Peters (2005) showed that the APS 3321 is capable of accurate sizing and has 85–100% counting efficiency for solid particles between 0.8 and 10 μm. Consequently, the APS may be used as a reference to evaluate the performance of other real-time instruments, such as the PASs, for the measurement of dry aerosols.

Thus, the objective of the current work was to compare the performance of the PAS 1.108 and the PAS 1.109 with that of the APS 3321. Performance was evaluated in terms of sizing and counting for monodisperse and polydisperse solid aerosols. Comparisons included both number concentration by size and mass concentration by size for polydisperse aerosols.

MATERIALS AND METHODS

Experimental setup

Figure 1 provides a schematic diagram of the experimental setup. Aerosol was introduced into air cleaned with high-efficiency particulate air (HEPA) filters and mixed with a 6 inches box fan in the upper section of a 1 m^3 vertical flow chamber. The flow rate through the chamber was maintained below 0.19 m^3 min^{-1}, which resulted in a maximum downward moving face velocity of 0.003 m sec^{-1}. This face velocity was less than the criteria of <0.1 m s^{-1} used by others for 'very slow moving air' (Witschger *et al*., 2004). The diluted aerosol was then passed through a baffle that provided sufficient pressure drop to force a uniform velocity profile as it entered the lower test section of the chamber.

As shown in Table 1, the aerosol was measured in the lower section of the chamber with three real-time instruments: one PAS 1.108 (Grimm Technologies, Inc.); one PAS 1.109 (Grimm Technologies, Inc.); and one APS 3321 (TSI Incorporated, Shoreview, MN, USA). Whereas the PAS 1.108 measures particle number concentration by size from 0.3 to 20 μm in 15 channels, the PAS 1.109 provides similar information over a slightly greater size range at double the resolution (0.2–20 μm in 30 channels). Compared to the PASs, the APS provides information over a slightly narrower size range (0.5–20 μm) and costs substantially more (roughly 4 times more than the PAS 1.108 and 2 times more than the PAS 1.109). A stainless steel tube (4 mm OD × 3 mm ID) provided by the manufacturer was used as the inlet for the PASs. The inlet for the APS consists of an aluminum tube (18.9 mm OD × 15.9 mm ID). The airflow into the inlets was aligned with gravity.

The PAS instruments were calibrated by the manufacturer prior to starting these experiments. The following outlines the calibration procedures performed by Grimm Technologies, Inc. A calibration curve is developed by relating the particle mass concentration indicated by the instrument being calibrated to a reference unit while both units measure polydisperse NBS-standard Dolomite dust over a broad size range. The reference unit is calibrated by size with NIST-traceable PSL spheres

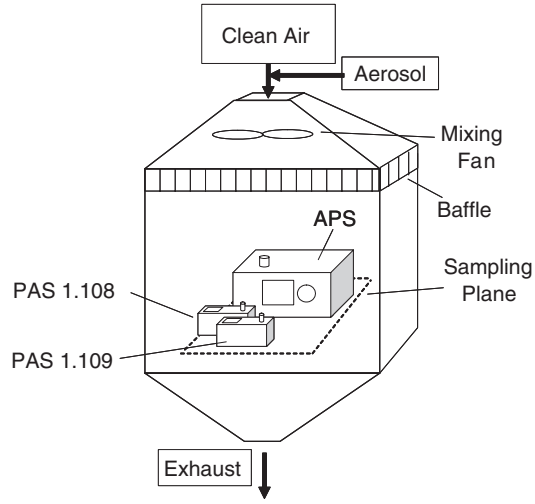

Fig. 1. Schematic diagram of the experimental setup.

Table 1. Manufacturer reported capabilities of each instrument evaluated

	Grimm PAS 1.108	Grimm PAS 1.109	TSI APS 3321
Measurement principal	Optical	Optical	Optical and time-of-flight
Size range (μm)	0.3–20	0.25–32	0.5–20
Number of channels	15	31	52
Max number conc. (particles cm^{-3})	2000	2000	1000
Max mass conc. (mg m^{-3})	100	100	Not reported

and checked that it properly measures the NBS-standard Dolomite dust. The obtained mean mass from the reference unit is regularly compared with a high-volume, filter-based sampler at the factory for any drift in calibration (Grimm, personal communication).

The APS unit was relatively new and had been calibrated by the manufacturer within 6 months prior to these experiments. When TSI Incorporated calibrates the APS, the sheath air flow rate is set to 4.00 ± 0.05 Lpm, and the aerosol flow rate is set to 1.00 ± 0.05 Lpm. The optics are then aligned until the APS-indicated particle concentration is within 10% of that measured with a condensation particle counter (M/N 3010; TSI Incorporated) for a 0.70 μm PSL aerosol. A calibration curve is then developed by relating the time-of-flight of 11 different monodisperse aerosols composed of PSL spheres that range in size from 0.36 to 20 μm. The calibration curve is then uploaded to the firmware of the APS.

PROCEDURES

Tests were conducted with monodisperse and a polydisperse aerosols. A nebulizer (Cat. 002002, Airlife Nebulizer, Allegiance Healthcare Corp., McGraw Park, IL 60085, USA) operated at 10 psig was used to spray a suspension of monodispersed PSL spheres (Duke Scientific Corp., Palo Alto, CA, USA) in distilled water. Tests were conducted with three sizes of fluorescently tagged, green PSL spheres with manufacturer-reported diameters of 0.83, 1 and 3 μm. A further test was conducted with white PSL spheres with a manufacturer-reported diameter of 1 μm to investigate the effect of PSL color on instrument performance. The manufacturer of the PSL provided certification that the mean diameters of the PSL spheres was within 0.03 μm of the stated particle diameter and that the coefficient of variation of the size distribution of the spheres was <1.1% as determined by NIST-traceable microscopic methods. The concentration of the PSL in the chamber was maintained at 100 particles cm^{-3} by altering the clean air flow to the chamber.

A polydisperse aerosol was generated by aerosolizing Arizona test dust (ISO Medium, 12103-1, A3; Powder Technology Incorporated, Burnsville, MN, USA) with a Wright dust feeder (Wright Dust Feeder II; BGI, Inc., Waltham, MA, USA). The parameters pertinent to this work for Arizona test dust were as follows: refractive index = 1.5 (O'Shaughnessy and Slagley, 2002); particle density, ρ_p = 2.65 g cm^{-3} (Endo *et al.*, 1998); and particle aerodynamic shape factor, χ = 1.5 (Endo *et al.*, 1998). The dust feeder was operated to maintain the particle number concentration between 500 and 1000 particles cm^{-3} as measured with the APS.

The aerosol number concentrations in both monodisperse and polydisperse tests were maintained <1000 particles cm^{-3} to avoid errors associated with particle coincidence. Particle coincidence error is when two or more particles enter the sensing zone of the instrument at the same time and leads to improper sizing. The PASs incorporate an algorithm to accommodate for particle coincidence for particle number concentration up to 2000 particles cm^{-3} (Grimm, personal communication). Models of the APS earlier than that tested in this work suffered from severe particle coincidence errors and the generation of 'phantom' particles due to signal processing issues (Heitbrink and Baron, 1991). These issues were compounded by other erroneous counts that were created when particles recirculated through the sensing zone of the APS rather than properly being routed through its exit (Stein *et al.*, 2002). Many of the signal processing coincidence issues were resolved when TSI introduced the Model 3320 (Holm *et al.*, 1997), and the problem of recirculation was resolved in the current APS Model 3321 (Peters and Leith, 2003; Volckens and Peters, 2005). The effective number concentration to avoid coincidence issues is now stated to be 1000 particles cm^{-3} by TSI Incorporated.

The instruments were set to report a size distribution every 6 s. For each test aerosol, the particle concentration in the chamber was monitored with the APS until it was stable to within ±10% of the desired concentration. The instruments were then used to measure the aerosol in the chamber for a period of 10 min. Each PSL aerosol was measured three times and the polydisperse aerosol five times to estimate measurement precision. Prior to testing, the spatial uniformity of aerosol in the chamber was evaluated by measuring particle number concentration by size in the four corners of the chamber. These tests showed that the size distributions were nearly identical and the coefficient of variation in particle number concentration was <10% among the four locations.

DATA ANALYSIS

For monodisperse aerosol, the particle number distribution was scanned to identify the channels containing PSL sphere counts. The particle number mode diameter was estimated as the arithmetic midpoint diameter of the channel with the maximum particle number concentration. The total number concentration was estimated as the sum of the particle number concentration observed in all channels containing sphere counts. The mode diameter and number concentration measured with the three instruments were then compared.

For polydisperse dusts, the particle number concentration by size measured with each instrument was

converted to mass concentration by size. For these conversions, it was assumed that the optical particle size measured by the PAS was equivalent to the volume equivalent or geometric diameter of the particle and the APS measured the aerodynamic diameter of the particle. For the PASs, the differential mass concentration in each size channel, dM_i, was calculated as follows:

$$dM_i = \frac{\pi}{6} D_{ve,i}^3 \rho_p dN_i \quad (1)$$

where $D_{ve,i}$ is the volume-equivalent midpoint diameter of the i-th channel and dN_i is the number concentration measured in the i-th channel. The aerodynamic diameter for the midpoint of each size channel of the PAS was then calculated as:

$$D_{ae,i} = D_{ve,i} \sqrt{\frac{\rho_p C_{ve,i}}{\rho_0 C_{ae,i} \chi}} \quad (2)$$

where D_{ae} is aerodynamic diameter, D_{ve} is the arithmetic volume equivalent midpoint diameter, ρ_0 is unit density (1 g cm^{-3}), C_{ae} is the Cunningham correction factor associated with the aerodynamic diameter and C_{ve} is the Cunningham correction factor associated with the volume equivalent diameter.

The APS directly measures particle aerodynamic diameter. To calculate mass concentration, the arithmetic midpoint aerodynamic diameter was first converted to the volume equivalent diameter for each APS channel using Equation 2 solved for D_{ve}. Differential mass concentration for a given aerodynamic diameter ($dM_{D_{ae}}$) was then calculated for each channel of the APS as follows:

$$dM_{D_{ae}} = dN_{D_{ae}} \frac{\pi}{6} D_{ve}^3 \rho_p. \quad (3)$$

A macro in a spreadsheet (Visual Basic macro in Excel; Microsoft, Redmond, WA, USA) was created to perform the iterative calculations needed to solve Equation 2 containing the Cunningham correction factor which is dependent on diameter.

RESULTS AND DISCUSSION

Monodispserse aerosols

Table 2 provides a summary of the tests conducted with aerosols composed of monodisperse PSL. For the 1.0 μm spheres, the number mode diameters measured with different instruments were the same but was slightly smaller than the manufacturer-reported diameters. For the other two PSL aerosols, the number mode diameter measured with the PASs was smaller than that reported by the APS and further from the manufacturer-reported diameter. The number mode diameter measured with the PAS 1.108 was the same (0.90 μm) for both the 0.83 and 1.0 μm spheres.

Figure 2 shows the particle size distributions measured by each instrument for the 0.83 μm spheres. Although there appear to be clear differences in the way the instruments classified this aerosol, the discrepancies in sizing among instruments may be partially attributed to differences in their size resolution. Whereas the PAS 1.108 has 15 size channels, the PAS 1.109 has 31 channels and the APS has 52 channels. Unlike the PAS 1.108, the increased size resolution offered by the PAS 1.109 and APS enabled them to distinguish the 0.83 μm spheres from the 1.0 μm spheres.

As shown in Table 2, the number concentration measured with the PAS 1.109 was greater than that measured with the PAS 1.108, which in turn was greater than that measured with the APS, for all PSL sizes. The percent difference in number concentration between the PAS 1.109 and the APS increased with particle size from +23% at 0.83 μm to +59% at 3.0 μm. The percent difference in number concentration between the PAS 1.108 and the APS increased with particle size from +3% at 0.83 μm to +27% at 3.0 μm. The difference in response between the two PASs is unclear and warrants further investigation because both units were calibrated prior to testing by the manufacturer. In general, the positive bias between the counting efficiency of the PAS 1.108 and the APS is consistent with the data presented

Table 2. Summary of tests conducted with monodisperse PSL aerosol

Manufacturer-reported sphere diameter (μm)	Grimm PAS 1.108	Grimm PAS 1.109	TSI APS 3321
Number mode diameter (μm)			
0.83 μm	0.90	0.68	0.78
1.0 μm	0.90	0.90	0.90
3.0 μm	2.5	2.5	2.8
Mean number concentration ± standard deviation (particles cm^{-3})			
0.83 μm	3.2 ± 0.3	3.8 ± 0.4	3.1 ± 0.24
1.0 μm	0.67 ± 0.04	0.69 ± 0.02	0.54 ± 0.09
3.0 μm	0.028 ± 0.016	0.035 ± 0.018	0.022 ± 0.007

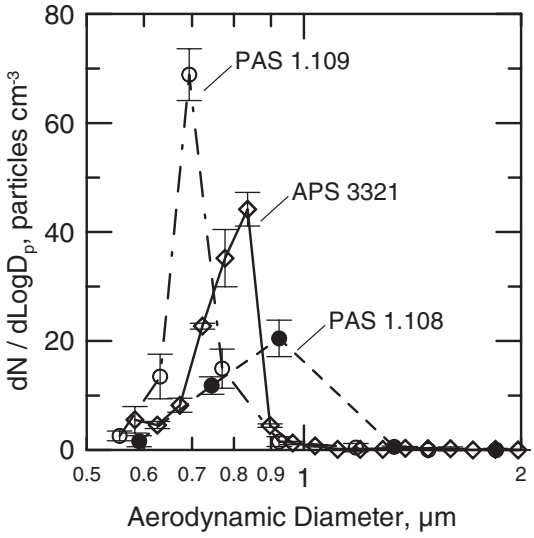

Fig. 2. Normalized particle size distributions measured for 0.83 µm PSL. Error bars represent 1 SD.

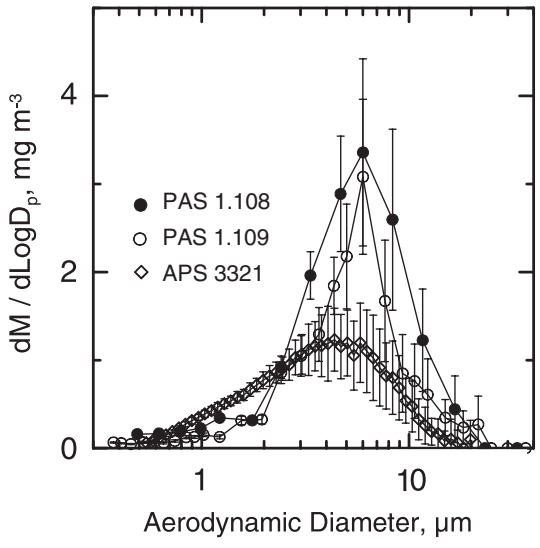

Fig. 4. Normailzed particle mass concentration by size measured for Arizona test dust. Error bars represent 1 SD.

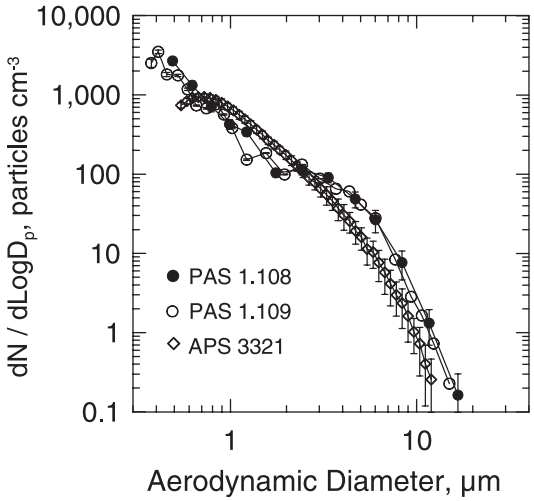

Fig. 3. Normalized particle number concentration by size measured for Arizona test dust. Error bars represent 1 SD.

in Volckens and Peters (2005). They observed that the counting efficiency of the APS deviated from 100% for PSL particles (92% for 0.83 µm, 85% for 1.0 µm and 98% for 3.0 µm particles). An additional experiment with a direct measure of particle number concentration would help to clarify these discrepancies.

Polydisperse aerosols

Figure 3 provides number histogram, and Fig. 4 provides the mass histogram measured for the Arizona test dust. Table 3 provides summary statistics for these data. As shown in Fig. 3, the number concentration by size measured with all instruments decreased from 800 particles cm^{-3} at 0.7 µm to below 1 particle cm^{-3} at 10 µm. For particles progressively smaller than 0.7 µm, the number concentration measured with the PASs increased, whereas that measured with the APS decreased. For particles between 0.7 and 2 µm in size, the number concentration measured with the PASs was substantially less than that measured with the APS. Additionally, whereas the number distribution measured with the PASs decreased sharply and then flattened at 2 µm, which measured with the APS resulted in a smooth decline. The number concentration measured with the PASs was greater than that measured with the APS for particles larger than 2.5 µm.

As shown in Fig. 4, the mass concentration by size measured with different instruments was similar, with some notable deviations. The mass concentration distribution measured with the PASs was shifted to slightly larger sizes when compared with that measured with the APS. For particles larger than 2.5 µm, the mass concentration measured with the PASs was greater than that measured with the APS. These observations are reflected in the summary statistics compiled in Table 3. The high number concentrations observed in the smallest channels of the PASs (Fig. 3) account for the greater total number concentration measured with the PASs compared to that measured with the APS. The number concentration in the small channels of the PASs also tended to make the number distribution more broad (greater geometric standard deviation) and skew it to smaller sizes (smaller number median diameter) when compared with the APS.

The PASs were capable of detecting smaller particles than the APS. Several researchers have

Table 3. Summary of tests conducted with Arizona test dust

Parameter	Grimm PAS 1.108 (average ± standard deviation)	Grimm PAS 1.109 (average ± standard deviation)	TSI APS 3321 (average ± standard deviation)
By number			
Number median diameter, μm	0.48 ± 0.01	0.51 ± 0.01	0.86 ± 0.09
Geometric standard deviation	2.44 ± 0.06	2.31 ± 0.07	1.91 ± 0.09
Total concentration, particles cm^{-3}	674 ± 79	749 ± 91	429 ± 84
By mass			
Mass median diameter, μm	4.5 ± 0.5	4.4 ± 0.4	3.3 ± 0.34
Geometric standard deviation	2.18 ± 0.04	2.16 ± 0.07	2.02 ± 0.11
Total concentration, mg m^{-3}	1.98 ± 0.56	1.35 ± 0.40	0.99 ± 0.26
Respirable mass concentration, mg m^{-3}	0.97 ± 0.16	0.52 ± 0.10	0.53 ± 0.10

documented that the counting efficiency of the APS becomes progressively <100% for particles smaller than 0.7 μm (Kinney and Pui, 1995; Armendariz and Leith, 2002). Thus, the particle number concentration measured by the PASs between 0.3 and 0.7 μm were probably closer to the true concentration than that of the APS. The better detection capability of the PASs for small particles over the APS may be attributed to the optical method of counting and sizing.

The lower number concentration measured by the PASs compared with the APS between 0.7 and 2 μm presents a challenge to interpret. These data are opposite of those presented for PSL in Table 2, where the number concentration measured with the PASs was greater than that measured with the APS. These results may be explained by differences in optical characteristics of the spherical PSL particles and the irregularly-shaped Arizona test dust particles. Alternatively, impaction on the tip of and/or shearing within the acceleration nozzle of the APS may provide sufficient force to break apart agglomerated Arizona test dust particles. If true, a single large particle would be broken into two or more smaller particles. This phenomenon would explain the fact that the PAS overestimated number concentration for particles larger than 2.5 μm but underestimated that for particles smaller than 2.5 μm. The data from the current experiments are insufficient to test this hypothesis further.

The aspiration of particles into the inlet of the instruments was considered as a possible bias to explain these differences. Theoretical aspiration, η, by size of the PAS and APS inlets was calculated as (Grinshpun *et al*., 1993):

$$\eta = \frac{V_{ts}}{U} * \cos(\varphi) + \exp\left(-\frac{4\mathrm{Stk}^{1+\sqrt{\frac{V_{ts}}{U}}}}{1+2\mathrm{Stk}}\right) \quad (4)$$

where V_{ts} is the terminal settling velocity of the particle, U is the sampling velocity, φ is the inlet axis with respect to gravity (φ = 0 for the upward-facing nozzle in this work), and Stk is the particle Stokes number based on the sampling velocity and the inlet

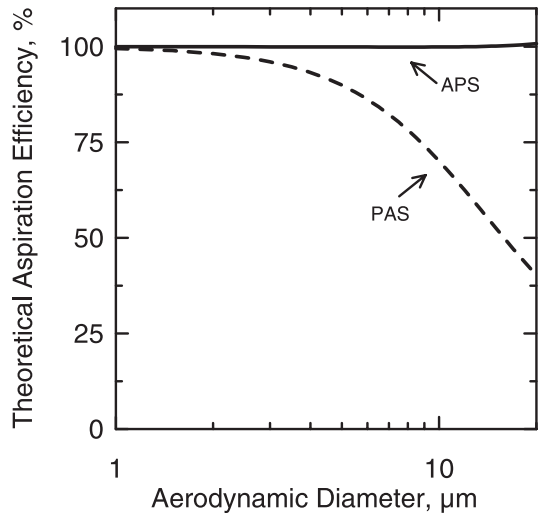

Fig. 5. Theoretical aspiration efficiency for the inlet tube of the PAS and the APS oriented vertically and in calm air.

diameter. The sampling velocity was based on the outer diameter of the inlet because they are beveled from the outside to inside in both the PAS and APS. The sampling velocity was calculated for the APS to be 29.7 cm s^{-1} based on flow rate of 5 Lpm and an outer tube diameter of 1.89 cm, and for the PAS to be 159 cm s^{-1} based on flow rate of 1.2 Lpm and an outer tube diameter of 0.4 cm. As mentioned, the air in the test section of the chamber used in this work approximated the calm air conditions for which Equation 4 was based.

As shown in Fig. 5, whereas the theoretical aspiration of the APS was near 100% for particles as large as 20 μm, that of the PAS became progressively less than 100% as particle size became larger than 1 μm. This deviation occurred due to the second term in Equation 4, which represents the combined effect of inertia and gravity on aspiration. For a 20 μm particle, the Stokes number indicated that particle inertia is negligible for aspiration into the APS (Stk = 0.04) but not for the PAS (Stk = 0.49). However, these theoretical results are opposite to the

experimental observation, where particle mass concentration estimated with the PASs above 2 μm was substantially greater than that estimated with the APS (Fig. 3). The reason for this discrepancy is unknown.

Further experiments are needed to clarify the observations made in this work. Specifically, an experiment designed to directly assess the detection efficiency of the PASs by size would help to interpret differences observed between the PASs and the APS. Tests at different aerosol concentrations would also be informative. Further experiments are also needed to compare the performance of these instruments with liquid aerosols. Measurement of liquid aerosols with the APS is problematic for several reasons: droplets deform during acceleration and are sized to small (Cheng *et al*., 1986; Chen *et al*., 1990; Bartley *et al*., 2000); and droplets are not detected with 100% efficiency because they impact on the acceleration nozzle (Volckens and Peters, 2005). The PASs should be unaffected by these acceleration-related issues but may be biased by the refractive index of different liquids.

CONCLUSIONS

This study compared the response of two optical particle counters, the PAS 1.108 and the PAS 1.109, with that of the APS 3321 for dry particles: three sizes of monodisperse PSL spheres (0.83, 1.0 and 3.0 μm) and a polydisperse aerosol (Arizona test dust). For PSL aerosols, the number mode diameters measured with the PASs were similar to those measured with the APS. The number concentration measured with the PASs was greater than that measured with the APS.

For polydisperse aerosol, the PASs provided similar results to those from the APS. However, there were systematic differences among instruments in number and mass concentration measurement that depended upon particle size. The PASs were able to detect particles with greater efficiency than the APS for particles smaller than 0.7 μm. Although number concentration reported by the PAS 1.108 and PAS 1.109 were both greater than the APS in monodisperse tests, they were lower than the APS in polydisperse tests for particles between 0.7 and 2 μm. The experiments conducted in this work were insufficient to resolve these differences.

REFERENCES

Armendariz AJ, Leith D. (2002) Concentration measurement and counting efficiency for the aerodynamic particle sizer 3320. J Aerosol Sci; 33: 133–48.

Baron PA, Mazumder MK, Cheng YS. (2001) Direct-reading techniques using particle motion and optical detection. In Baron PA, Willeke K, editors. Aerosol measurement: principles, techniques, and applications. New York: Wiley-Interscience.

Bartley DL, Martinez AB, Baron PA *et al.* (2000) Droplet distortion in accelerating flow. J Aerosol Sci; 31: 1447–60.

Chen BT, Cheng YS, Yeh HC. (1990) A study of density effect and droplet deformation in the TSI aerodynamic particle sizer. Aerosol Sci Technol; 12: 278–85.

Cheng YS, Chen BT, Yeh HC. (1986) Size measurement of liquid aerosols. J Aerosol Sci; 17: 803–9.

Cohen AJ, Ross Anderson HB, Ostro KD *et al.* (2005) The global burden of disease due to outdoor air pollution. J Toxicol Environ Health; 68: 1301–7.

Colls JJ, Micallef A. (1999) Measured and modelled concentrations and vertical profiles of airborne particulate matter within the boundary layer of a street canyon. Sci Total Environ; 235: 221–33.

D'Ippoliti DF, Forastiere C, Ancona N *et al.* (2003) Air pollution and myocardial infarction in Rome: a case-crossover analysis. Epidemiology; 14: 528–35.

Endo YD, Chen D-R, Pui DYH. (1998) Bimodal aerosol loading and dust cake formation on air filters. Filtration Sep; 35: 191–5.

Gebhart J. (2001) Optical direct-reading techniques: light intensity systems. In Baron PA, Willeke K, editors. Aerosol measurement: principles, techniques, and applications. New York: Wiley Interscience.

Grinshpun SK, Willeke K, Kalatoors S. (1993) A general equation for aerosol aspiration by thin-walled sampling probes in calm and moving air. Atmos Environ; 27A: 1459–70.

Hall RM, Heitbrink WA, Reed LD. (2002) Evaluation of a tractor cab using real-time aerosol counting instrumentation. Appl Occup Environ Hyg; 17: 47–54.

Heitbrink WA, Baron PA. (1991) Coincidence in time-of-flight aerosol spectrometers: phantom particle creation. Aerosol Sci Technol; 53: 427–531.

Hinds WC. (1999) Aerosol technology: properties, behavior, and measurement of airborne particles. New York: John Wiley & Sons, Inc. pp. 242–8.

Holm RL, Caldow R, Hairston PP *et al.* (1997) An enhanced time-of-flight spectrometer that measures aerodynamic size plus light-scattering intensity. J Aerosol Sci; 28(Suppl 1): S11–2.

Janssen NA, Schwartz J, Zanobetti AH *et al.* (2002) Air conditioning and source-specific particles as modifiers of the effect of PM(10) on hospital admissions for heart and lung disease. Environ Health Perspect; 110: 43–9.

Kinney PD, Pui DYH. (1995) Inlet efficiency study for the TSI aerodynamic particle sizer. Part Part Syst Charact; 12: 188–93.

O'Shaughnessy PT, Slagley JM. (2002) Photometer response determination based on aerosol physical characteristics. AIHA J (Fairfax, Va); 63: 578–85.

Peters TM, Leith D. (2003) Counting efficiency of the model 3321 aerodynamic particle sizer. Proceedings of the 22nd Annual American Association of Aerosol Researchers Conference, Anaheim, CA, USA.

Peters AD, Dockery W, Muller JE *et al.* (2001) Increased particulate air pollution and the triggering of myocardial infarction. Circulation; 103: 2810–5.

Peters TM, Heitbrink WA, Evans DE *et al.* (2005) The mapping of fine and ultrafine particle concentrations in engine machining and assembly plant. Ann Occup Hyg; Available online at http://annhyg.oxfordjournals.org.

Schlesinger RB, Kunzli NG, Hidy M *et al.* (2006) The health relevance of ambient particulate matter characteristics: coherence of toxicological and epidemiological inferences. Inhal Toxicol; 18: 95–125.

Stein S, Gabrio G, Oberreit D *et al.* (2002) An evaluation of mass-weighted size distribution measurements with the

model 3320 aerodynamic particle sizer. Aerosol Sci Technol; 36: 845–54.

Teikari M, Linnainmaa M, Laitinen J *et al.* (2003) Laboratory and field testing of particle size-selective sampling methods for mineral dusts. AIHA J (Fairfax, Va); 64: 312–8.

Volckens J, Peters TM. (2005) Counting and particle transmission efficiency of the aerodynamic particle sizer. J Aerosol Sci; 36: 1400–8.

Wellenius GA, Schwartz J, Mittleman MA. (2005) Air pollution and hospital admissions for ischemic and hemorrhagic stroke among medicare beneficiaries. Stroke; 36: 2549–53.

Witschger O, Grinshpun SA, Fauvel S *et al.* (2004) Performance of personal inhalable aerosol samplers in very slowly moving air when facing the aerosol source. Ann Occup Hyg; 48: 351–68.